International Journal of Technology (2012) 2: 129-139
ISSN 2086-9614

INVESTIGATION OF PHOTOELECTRODE MATERIALS INFLUENCES IN TITANIA-BASED-DYE-SENSITIZED SOLAR CELLS

Natalita M. Nursama*, Lia Muliani

Research Center for Electronics and Telecommunication – Indonesian Institute of Sciences (LIPI)
Kampus LIPI Jl. Sangkuriang Building 20 4th floor, Cisitu
Bandung 40135, Indonesia

(Received: March 2012/ Revised: June 2012 / Accepted: July 2012)

ABSTRACT

Solar cells are excellent devices which enable the provision of renewable energy in a safe and easy way. A dye sensitized solar cell (also referred as dye solar cell) is a new type of solar cell, whose operation is based on photoelectronic chemically activated mechanism. The fabrication of dye sensitized solar cells is generally simpler and cheaper compared to the conventional silicon-based solar cells. This paper aims to fabricate and analyze the performance of dye solar cell by comparing the utilization of transparent and opaque TiO_2 pastes for the photoelectrodes. In addition, we also perform an analysis on the use of two different red ruthenium based dye, i.e. N-719 and Z-907. The current-voltage (I-V) measurements were performed by using an artificial sun-simulator on AM1.5 irradiation. As for the counter-electrode, platinum (Pt) was used as the catalyst which was deposited using DC-sputtering technique. Our results revealed that the cells featuring transparent TiO_2 paste achieved better photoconversion efficiencies compared to that of the opaque paste. The best average efficiency achieved was 3.78% for cells with a total active area of 2 cm^2. In addition, transparent cells produced on average up to 3 mA higher photocurrent compared to that of the opaque cells. We suspected that such behavior was affected by the discrepancy in the crystallite size.

Keywords: Dye; Photoelectrode; Solar cell; TiO_2; Titania

1. INTRODUCTION

The increasing energy demand has been promoting the creation of devices that are able to convert alternative source of energy, such as solar energy. Solar cells can substantially reduce greenhouse gas emissions by converting solar energy into electricity. The Dye-sensitized Solar Cell (DSC) is a third generation solar cell which employs the basic mechanism of photoelectron chemistry to produce electricity. Since the work on this device was firstly reported by Gratzel and his co-workers in 1991 (O'Regan & Gratzel, 1991), the DSC technology has been developed very quickly. This type of solar cell has been of interest among photovoltaic (PV) scientists and academics as it can be produced in lower-cost processes compared to the conventional solar cells, which are mostly fabricated from silicon. In addition to the low-cost factor, DSC is also attractive due to its stylish color design and its transparency.

The DSC design represents an abrupt change from traditional solid-state based solar cells. In DSC, the photo-electrode, sometimes also referred as working electrode, is made from nano-scale particles of titanium dioxide (TiO_2, also referred as titania), coated with monolayer of

*Corresponding author's email: natalita@ppet.lipi.go.id, Tel: +62-22 -2504660, Fax: +62-22-2504659

light-absorbing dye, which is similar to chlorophyll in green leaves. Some other variations, such as changing the semiconductor and electrolyte materials have been reported (Boschloo et al., 2006; Fujishima & Zhang, 2006). However, those that are close to commercial development generally include nanoparticles of titania and a liquid electrolyte containing a redox couple. The best nanocrysalline titania-based DSCs to date have been fabricated using screen printing deposition (Chiba et al., 2006; Yella et al., 2011) with efficiency levels over 11%. Screen printing is a widespread industrially-viable technique as it is able to provide a fast-printing process with relatively easy control parameters for thickness and position.

Figure 1 provides the schematic of the typical DSC physical structure. The configuration of a standard DSC consists of two sandwiched glass layers with a Transparent Conducting Oxide (TCO). One electrode features a porous titanium dioxide (TiO2) layer stained with dye molecules, identified as the photo-electrode, while the other is the counter-electrode in which platinum (or other catalysts) is used as the deposition process. After being sandwiched together, electrolyte layers of redox species (I- and I3-) exist between the two electrodes. The working principle of a DSC is based on kinetics of electron transfer reactions. The photoelectronic chemical mechanisms, which occur during electron transfer within the DSC are as follows: a dye molecule is excited upon photon (hυ) absorption, whereas the electron is excited from the highest occupied molecular orbital (HOMO - D) into the lowest unoccupied molecular orbital (LUMO – D*) as shown by Equation (1).

$$D + h\upsilon \rightarrow D^* \tag{1}$$

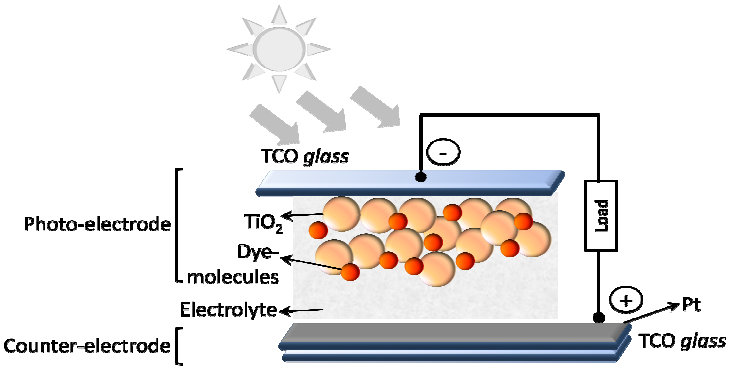

Figure 1 Basic structure of typical DSC

The free electron is subsequently injected into the conduction band of TiO_2 and transparent conducting oxide (TCO) towards the external circuit and the oxidized dye molecule D+ (2) is left.). When the electron reaches the catalyst layer (Pt or C), then it recombines with the holes within the electrolyte, in form of tri-iodide (I3-), to produce iodide ions (I-) through redox reactions. This reaction is shown by Equation (3). The negative charge of I- diffuses back into the dye and reacts with the oxidized molecule D+ and a full electrical cycle is therefore completed (See Equation (4)).

$$D^* \rightarrow D^+ + e^- \tag{2}$$

$$I_3^- + 2e^- \rightarrow 3I^- \tag{3}$$

$$3I^- + 2D^+ \rightarrow I_3^- + 2D \tag{4}$$

In DSCs, the essential factor to an efficient light harvesting mechanism is the high surface area of porous titania films. Nanostructured titania films could provide enough surface area for more than 1000 dye monolayers compared to a flat titania film (Lenzmann & Kroon, 2007). Therefore, determination of photoelectrode materials is crucial because these components significantly affect photon absorption and, therefore, affect current generation within the cell. For titania materials, the crystal phase of TiO_2 particle used in DSC is generally in anatase nanoparticles because of their high absorbance upon dye additives (Saga, 2006). In its application, there are normally two types of TiO_2 pastes, i.e. transparent and opaque. In this paper, we compared the performances of DSC featuring these types of TiO_2 in terms of their optical and electrical properties. Similar to titania, the dye element also holds a great influence with respect to the current generation as well as on the visual appearance of the DSC itself. Therefore, we also provide analytical studies of DSCs using two different dye sensitizers, i.e. N-719 or [RuL2(NCS)2] 2 TBA, ($C_{58}H_{86}N_8O_8RuS_2$) and Z-907 or RuLL'(NCS)21, ($C_{42}H_{52}N_6O_4RuS_2$). The molecular structures of these dyes are shown in Figure 2. These two types of TiO2 and sensitizing dyes are commercially available materials that are most frequently applied in DSCs. However, most researchers normally apply one certain type of material in order to fabricate their DSCs, and yet, there are no direct comparisons made to compare their influence upon photoelectrode characteristics to date. Therefore, we aim to provide a comprehensive study to compare the performance of DSC photoelectrode upon the variation of these materials

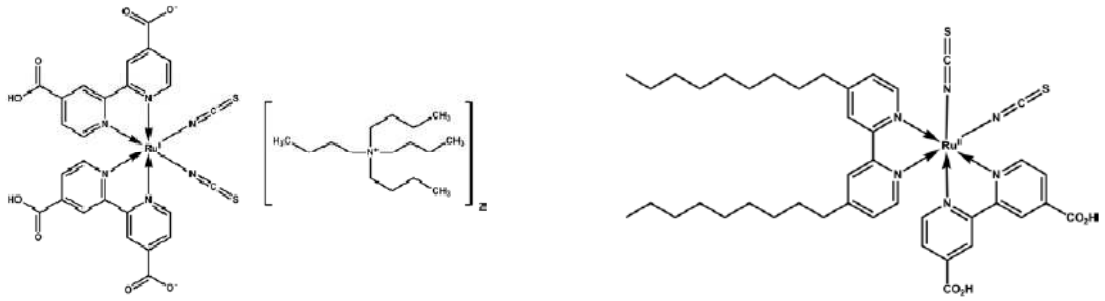

(a) (b)

Figure 2 Molecular complexes of Ruthenium based dye: (a) N-719; and (b) Z-907 (Dyesol, 2011)

2. EXPERIMENTAL

2.1. Preparation of photo-electrode

The conducting glass substrates used for both counter-electrodes and photo-electrodes were fluorine-doped tin oxide (SnO_2:F) from Dyesol, Australia with a conductivity of 15Ω/□. TiO_2 deposition process used a screen-printing technique with a Nylon #325 mesh. The printing was performed on an area of 20×10 mm^2. The samples were categorized into two different groups based on the titania types. The TiO_2 pastes used in the first group were Dyesol 18NR-AO with an opaque sintered layer and the other was 18NR-T with a transparent sintered layer. The printing process was performed twice, whereas each step ended with drying in an oven at a temperature of 175^{o}C for 10 minutes. At the end of the process, all samples were sintered on a conveyor-belt furnace at 450^{o}C for 15 minutes. Figure 3 shows the samples after being sintered at an elevated temperature.

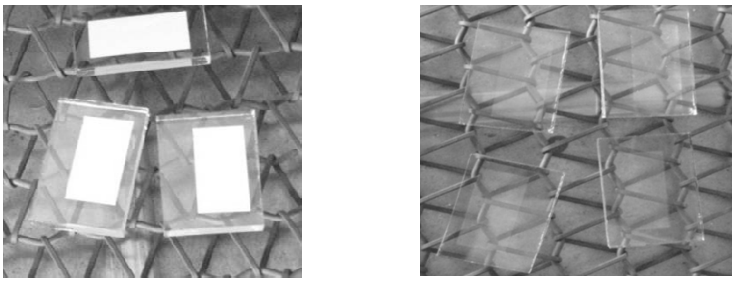

(a) (b)

Figure 3 Photo-electrodes of: (a) Opaque; and (b) Transparent titania films following a sintering at 450^{o}C

All samples were subsequently immersed on a solution consisting of ruthenium dye solution. One group from each titania sample group was dyed in B2(N719), while the other received the same treatment in DNH2(Z907). Both dye solutions were diluted in ethanol (C_2H_6O) with a concentration of 20 mg/100 ml. The dyeing process lasted for 24 hours on a dark place at room temperature and, in the end of the process; all samples were rinsed with ethanol to remove the dye residues or any existing water vapor. Following immersion, the TiO_2-coated electrodes turned to a maroon-black color (see Figure 4).

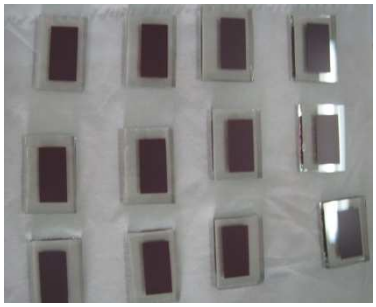

Figure 4 Titania based photo-electrodes after dyeing

2.2. Preparation of counter-electrode

The catalyst material used as the counter-electrode for our samples is platinum (Pt). The reason for selecting sputtered-Pt as the catalyst has been explained in our previous works (Nursam et al., 2011a; Muliani & Nursam, 2011). The Deposition process for the counter-electrode, was performed using DC-sputtering process with an initial pressure of 6.6×10^{-3} Pa, argon gas pressure of 5.3×10^{-1} Pa, rotation speed 5 rpm and power 5 W, for 20 minutes.

2.3. Cell assembly

Both photo-electrodes and counter-electrodes were assembled into a sandwich structure using thermoplastic sealant (Surlyn) with a thickness of 50 µm as the spacer, which is being attached on the TiO_2's surroundings. All samples were subsequently heated on a temperature of 120^{o}C to strengthen the attachment process. Finally, Dyesol liquid electrolyte EL-HSE was injected into the assembled samples and the remaining air holes were subsequently sealed using hermetic sealing compounds (also referred as glass frit). The application of glass frit as sealing material has been shown to improve the stability of liquid electrolyte-based DSCs for relatively long periods of time (Nursam et al., 2011b; Sastrawan et al., 2006). The final prototypes of DSC cells from this experiment are shown in Figure 5.

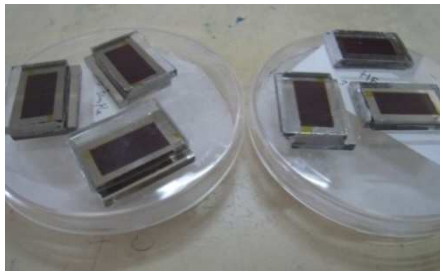

Figure 5 Titania-based DSC prototypes

2.4. Current-voltage characterization

Solar cell characterization is generally performed based on current-voltage (I-V) measurements using one-diode model. In our research, the I-V characterizations were done by measuring voltage when the DSC was illuminated and connected to a potentiometer with certain resistances. Other parameters that are also essential in characterizing solar cells are open-circuit voltage (Voc), short-circuit voltage (Isc), and efficiency. The photo-conversion efficiency can be calculated using following expression:

$$\%\eta = \frac{V_{OC} I_{SC} FF}{P_{in}} \times 100\% \quad (5)$$

Where P_{in} is the amount of lower received by the cell (measured using pyranometer) and FF is the fill factor which represents the quality of any solar cell's characteristics and is determine by the expression on Equation (6). The electrical circuit configuration that was used to measure the I-V data is shown in Figure 6.

$$FF = \frac{P_{\max}}{V_{OC} I_{SC}} \quad (6)$$

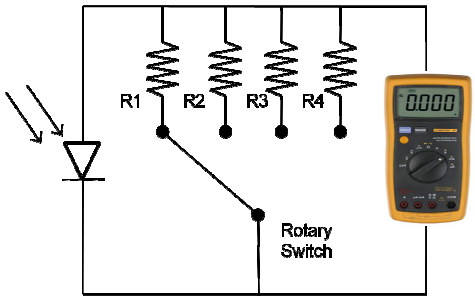

Figure 6 Electrical circuit diagram for *I-V* characterization

3. RESULTS AND DISCUSION

Figure 7 shows the scanning electron microscopy (SEM) images of TiO_2 layers with different transparency. The film surface morphologies shown by these SEM figures are those obtained after same sintering condition, i.e. 15 minutes at 450^{o}C. Annealing process at elevated temperature changed the particle size and structure into denser form. Each pore was diffused with the adjacent pores so that the porosity of the film was reduced. From Figure 7, it can be seen that large aggregates with less uniformity were found in the transparent layer with a broad pore distribution, while the opaque seem to disperse with better uniformity. We suspect that the

large clustering shown in our transparent photo-electrode is affected by the annealing condition. In our previous work, we report that the best photoconversion efficiency for an opaque TiO_2 electrode is achieved when annealing was performed at 450^{o}C (Muliani et al. 2010). Such condition, however, may not give an optimum result when it comes to transparent film. Thus, further optimization is necessary.

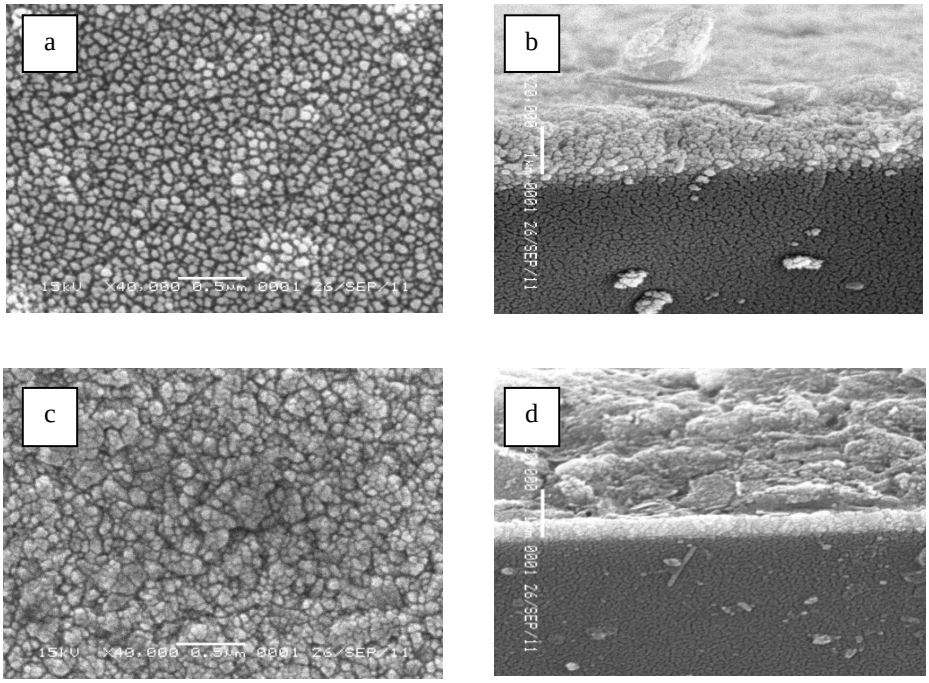

Figure 7 SEM images of TiO_2 particles with opaque: (a) top-view; (b) cross-section, and transparent: (c) top-view; (d) cross section layer

Further analysis on the physical structure of opaque and transparent TiO_2 particles is shown by the X-ray diffraction spectra provided in Figure 8. The XRD measurement was performed under radiation of Cu Kα 1.54060 Å (25 mA, 40 kV). Based on the diffractograms shown, it can be seen that both TiO_2 crystallites are in the anatase phase whereas the highest peaks of both TiO_2 were found at (101) crystal plane. Scherrer formula in the following equation was used to calculate the lower bound of the particle grain size.

$$\tau = \frac{k\lambda}{\beta \cos\theta} \tag{7}$$

Where τ is the mean size of the crystals, *k* is the shape factor (with typical value around 0.9), λ is the x-ray wavelength, β is the line broadening at half the maximum intensity (FWHM), and θ is the Bragg angle. The calculation result shows that crystallite size of TiO_2 transparent particles was around 17 nm (at $2\theta=25.38^o$), while TiO_2 opaque particles possessed crystallite size of approximately 40 nm (at $2\theta=25.35^o$). One should note that these particle sizes are relatively larger than those compared to several published works with synthesized TiO_2 nanoparticles in the range of 10-20 nm (Gratzel, 2004) or even less than 10 nm (Jiu et al., 2007). The DSC performance somewhat depends on the size and crystalinity of the TiO_2 particles. Wang et al. (Wang et al., 2004) reported that the higher photoconversion efficiency

could be achieved by smaller TiO_2 particles due to the effectiveness in dye absorptions. Therefore, we suspect that the TiO_2 transparent particles would have a higher rate of absorption, which in turn generates a higher level of output current. This, however, would require electrical characterizations as further justification. We provided such analysis at the end of this section.

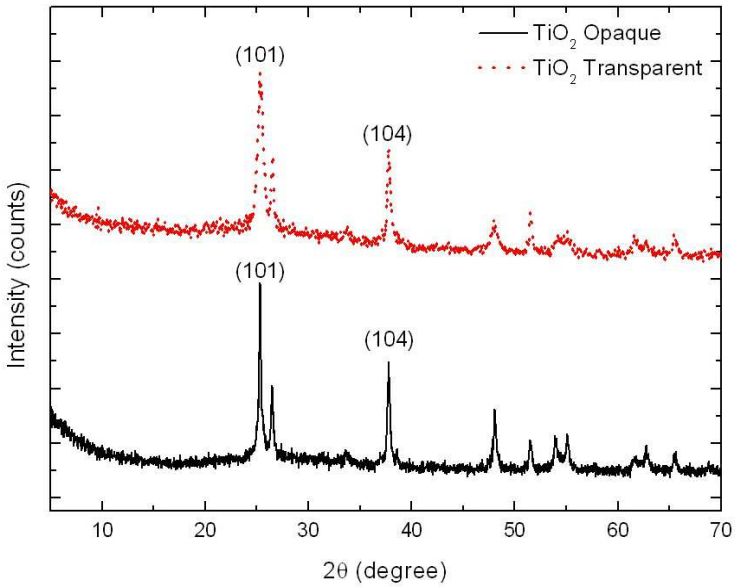

Figure 8 X-Ray diffraction spectra of TiO_2 films with opaque (black solid) and transparent (reddots) characteristics

One way of analyzing the effect of dye variations can be done by scrutinizing the optical characteristics of the dyes. Figure 9 shows the optical absorption of two different dyes as measured using a UV-VIS spectrophotometer. The measurement was performed directly upon each dye solution which had been dissolved in ethanol with a ratio of 1:5. It was observed that both dyes showed similar absorption patterns between the range of 400-700 nm, which fell within the visible light spectrum. However, it is clear that the average absorbance magnitude of N-719 is almost a factor of 2 times higher compared to the absorption spectra of dye Z-907.

Further UV-VIS spectrophotometer measurements were also performed to compare the optical characterizations between two types of TiO_2. Figure 10 shows the optical absorption of TiO_2 transparent and opaque particles. It can be seen that TiO_2 opaque generally has better absorption ability upon a broader wavelength interval. This could also be explained from the bandgap analysis. From the absorption spectrum in Figure 10, the bandgap energy (Eg) for each type of TiO_2 can be calculated using following expression:

$$E_g = \frac{hc}{\lambda} \tag{8}$$

Where h is the Planck constant (6.626×10^{-34} J/s), c is the speed of light (3×10^{8} m/s), and λ is the cut-off wavelength (m). From this calculation, we found that the bandgap energy of TiO_2 opaque ($\lambda_{cut\text{-}off}\approx700$ nm) and transparent ($\lambda_{cut\text{-}off}\approx380$ nm) particles are 1.78 eV and 3.27 eV, respectively. These bandgap values indicate that photon excitation in TiO_2 opaque occurs more easily compared to the photoconversion process in TiO_2 transparent, as implicated by its lower bandgap energy. With regards to our calculation using Scherrer formulation, these results

show that particle size is inversely proportional to bandgap, e.g. smaller particle size corresponds to bigger bandgap and vice versa.

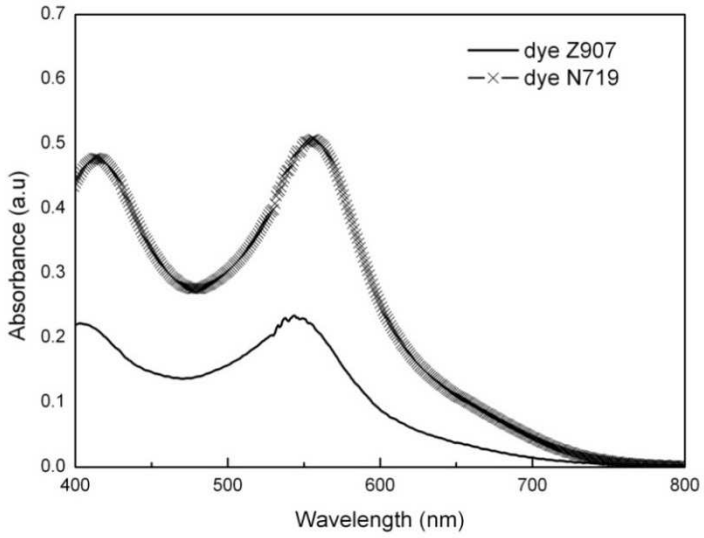

Figure 9 Light absorption spectra of dye N-719 and Z-907 solution, being diluted in ethanol

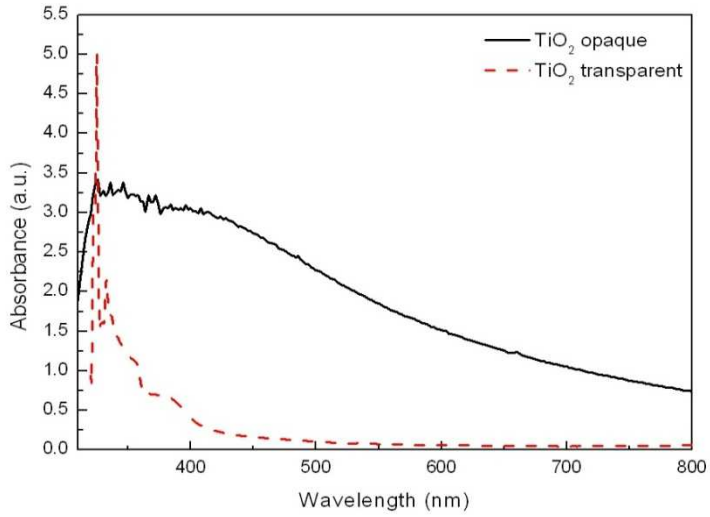

Figure 10 Light absorption spectra of TiO_2 opaque and transparent particles following annealing at 450^{o}C

Table 1 shows the summary of the output parameters whereas all the values provided were a function of the average value spread across all samples on the same group. Furthermore, Figure 11 shows the I-V characterization graph of our samples with various material combinations. There are several trends that can be observed. First, the general trend shows that samples

featuring transparent TiO_2 electrodes resulted in a better performance outcome, regardless of the dye type used, compared to those samples with non-transparent photoelectrodes. Transparent TiO_2 electrodes were shown to induce higher levels of photocurrent, photovoltage, and, thus, photoconversion efficiency. This is particularly profound when it comes to dye Z-907, as it can be seen from the combination of transparent TiO_2 electrodes. These additives have given the best results. (See Table 1 and Figure 11.) In the case of opaque TiO_2 electrodes, the effect of different dye hardly made any difference in the output performance. This is actually interesting considering that the light absorption of dye Z-907 was inferior compared to that of the N719 (see Figure 9). We suspect that the reason for this is due to the discrepancy in the dye characteristic itself, whereas Z-907 is hydrophobic and N-719 is hydrophilic. This result could be an indication that a hydrophobic dye was able to sensitize the TiO_2 layer at a higher degree of efficiency.

From our experiment, the best result, based on the photoconversion efficiency, was shown by the sample featuring transparent TiO_2 and dye Z907, with an efficiency reading of 4.41%. This was also represented by the highest average efficiency ratings compared to the rest of the group as shown in Table 1 (i.e. 3.78%). Cells featuring TiO_2 transparent particles on average produced up to 3 mA higher photocurrent compared to those of the opaque particles. It can be postulated that dye absorbance, which corresponds to light absorption in transparent TiO_2 particles has been working more effectively compared to the same process that occurs in opaque layer. Based on the Scherer's and bandgap calculation from XRD and UV-VIS measurements in this experiment, TiO_2 transparent film possessed smaller crystallite sizes with larger bandgap intervals compared to TiO_2 opaque particles. The fact that TiO2 transparent particles exhibited a higher output, irrespective of whether there was a higher bandgap, indicates that the particle size of the porous semiconductor holds an important key to improve the overall performance of DSC, especially at the current production levels. This also implies that the enhancement of light absorption is crucial. Smaller TiO_2 particles would result in a wider surface area, thus, absorbing more dye and improving light absorption.

Although the results of transparent TiO_2 electrode were better, it is generally difficult to promote the use of transparent TiO_2 electrodes within the structure used in this experiment as the finished cells were not actually transparent (due to the non-transparent Pt counter-electrode). Therefore we plan to perform further investigations on the optimization of transparent TiO_2 electrodes when combined with transparent Pt.

Table 1 Electrical parameters of DSC with TiO_2 photo-active area of 2×1 cm^2 (under AM1.5 with 40 mA/cm^2 illumination, R=1-3k3 Ω)

TiO_2 material	**Dye material**	**V_{OC} (mV)**	**I_{SC} (mA)**	**P_{max} (mW)**	***FF***	**η (%)**
Opaque	N-719	638	7.05	2.19	0.48	3.09
Transparent	N-719	652	7.23	2.57	0.55	3.67
Opaque	Z-907	611	7.50	2.13	0.47	3.09
Transparent	Z-907	668	8.90	2.84	0.47	3.78

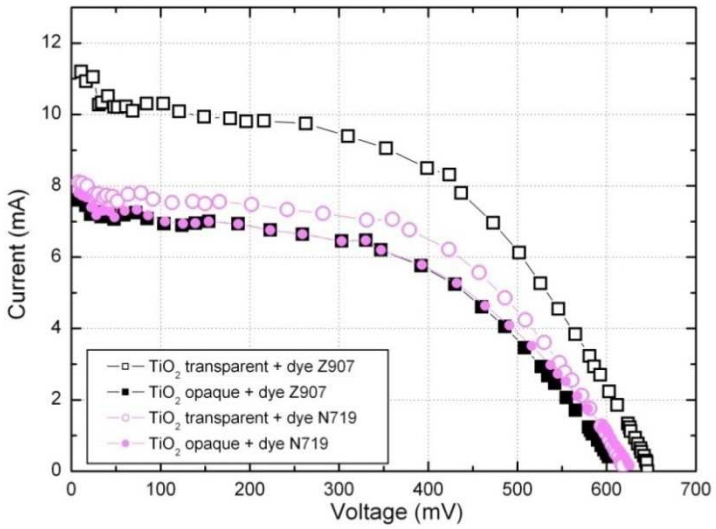

Figure 11 I-V characteristics of DSC with various TiO_2 and dye combinations (The curves shown were taken from the measurement results of the best sample).

4. CONCLUSION

This paper concerns the fabrication of dye solar cells (DSCs) with photo-electrodes made up of titania materials were prepared with a screen printing method in order to analyze the effect of TiO_2 and dye variations. Two types of TiO_2 photoelectrodes with different transparency characteristics were prepared under the same conditions. The SEM images showed that the transparent TiO_2 particles had relatively larger aggregates with less uniformity compared to that of the opaque TiO_2 film. However, the current-voltage characterization showed that the applications of transparent TiO_2 consistently produced higher output levels, particularly when applied with dye Z-907. This result was attributed to the particle size of the TiO_2 transparent which was smaller by a factor of 2 compared to the particle size of TiO_2 opaque, although TiO_2 opaque alone was able to absorb more photons due to its lower bandgap energy. We conclude that light absorption is essential, and therefore that the porous TiO_2 particle size is an important factor in improving the performance of DSC. The best average efficiency achieved in our experiment was 3.78%, which was shown by the sample featuring transparent TiO_2 and dye Z-907.

5. ACKNOWLEDGEMENTS

The authors greatly appreciate the support from Mr. Jojo Hidayat and Mr. Dede Ibrahim of PPET, Dr. Aminuddin of ITB, and Jono & Rahman of UNS Solo for the I-V and UV-VIS spectrophotometer measurements. This research was funded by the official budget of Indonesian Institute of Sciences (DIPA Tematik LIPI) year 2011

6. REFERENCES

Boschlolo, G., Edvinsson, T., Hagfeldt, A, 2006. Dye-sensitized nanostructured ZnO electrodes for solar cell applications. In T. Saga, (Ed), *Nanostructured materials for solar energy conversion*, pp. 227-254. Netherlands & UK: Elsevier.

Chiba, Y., Islam, Y., Watanabe, Y., Komiya, R., Koide, N., Han, L, 2006. Dye-sensitized solar cells with conversion efficiency of 11.1%, *Japanese Journal of Applied Physics*, Volume 45, No. 25, pp. L638-L640.

Dyesol Product Catalog March 2011. Retrieved from <http://www.dyesol.com/download/Catalogue.pdf> [January 26, 2012].

Fujishima, A., Zhang, X.T, 2006. Solid-state dye-sensitized solar cells. In T. Saga, (Ed), *Nanostructured materials for solar energy conversion*, pp. 255-273. Netherlands & UK: Elsevier.

Gratzel, M., 2004. Conversion of sunlight to electric power by nanocrystalline dye-sensitized solar cells, *Journal of Photochemistry and Photobiology A*: Chemistry, Volume 164, pp. 3-14.

Jiu, J., Isoda, S., Adachi, M., Wang, H., 2007. Dye-sensitized solar cell based on nanocrystalline TiO_2 with 3-10 nm in diameter. *Journal of Material Science: Materials in Electronics*, Volume 18, pp. 593-597.

Lenzmann, F.O., Kroon, J.M., 2007. Recent advances in dye-sensitized solar cells. *Advances in Optoelectronics*, Volume 2007, pp. 1-10.

Muliani, L., Taryana, Y., Hidayat, J., 2010. Pembuatan sel surya TiO_2 dye-sensitized menggunakan metoda screen printing, *Jurnal Elektronika dan Telekomunikasi*, Volume 10, No. 1, pp. 126-131.

Muliani, L., Nursam, N.M., 2011. Dye-sensitized solar cell based on carbon nanoparticle counter electrode. Proceedings of the 5th IMEN UKM-LIPI Joint Seminar on Microelectronics Devices, Systems, and Instrumentation 2011, Yogyakarta, November 16-17, Indonesia.

Nursam, N.M., Muliani, L., Hidayat, J., 2011a. Application of Pt counter electrode being deposited on TCO-free substrates for dye-sensitized solar cells. Proceedings of the 5th IMEN UKM-LIPI Joint Seminar on Microelectronics Devices, Systems, and Instrumentation 2011, Yogyakarta, November 16-17, Indonesia.

Nursam, N.M., Muliani, L., Hidayat, J., 2011b. Analyzing the effect of photoactive TiO_2 dimension and the encapsulation of dye-sensitized solar cells for solar energy conversion, *Teknologi Indonesia*, Volume 34, No. 2, pp. 85-92.

O'regan, B., Gratzel, M., 1991. A low-cost, high efficiency solar cell based on dye-sensitized colloidal TiO_2 films. *Nature*, Volume 353, pp. 737-740.

Saga, T., 2006. *Nanostructured Materials for Solar Energy Conversion*. Netherlands: Elsevier.

Sastrawan, R., Beier, J., Belledin, U., Hemming, S., Hinsch, A., Kern, R., Vetter, C., Petrat, F.M., Prodi-Schwab, A., Lechner, P., Hoffmann, 2006. A glass frit-sealed dye solar cell module with integrated series connection, *Solar Energy Materials and Solar Cells*, Volume. 90, pp. 1680-1691.

Wang, Z., Kawauchi, H., Kashima, T., Arakawa, H., 2004. Significant influence of TiO_2 photoelectrode morphology on the energy conversion efficiency of N719 dye-sensitized solar cell. *Coordination Chemistry Review*, Volume 248, pp. 1381-1389.

Yella, A., Lee, H.W., Tsao, H.N., Yi, C., Chandiran A.K., Nazeerudin, M.K, Diau, E.W., Yeh, C.Y., Zakeeruddin, S.M., Gratzel, M., 2011. Porphyrin-Sensitized solar cells with cobalt (II/III)–based redox electrolyte exceed 12% efficiency. *Science*, Volume 334, No. 6056, pp. 629-634.